RSC Advances

This article can be cited before page numbers have been issued, to do this please use: M. Akram, I. A. Bhat and P. K. ud-Din, *RSC Adv.*, 2015, DOI: 10.1039/C5RA20576J.

ROYAL SOCIETY OF CHEMISTRY

www.rsc.org/advances

View Article Online
DOI: 10.1039/C5RA20576J

New insights into binding interaction of novel ester-functionalized *m*-E2-*m* gemini surfactants with lysozyme: A detailed multidimensional study

Mohd. Akram*, Imtiyaz Ahmad Bhat and Kabir-ud-Din[a]

Department of Chemistry, Aligarh Muslim University, Aligarh-202002, India

*Corresponding author

E-mail address: drmohdakram@gmail.com

Tel.: +91 9411040048

[a]Present Address: Department of Chemistry, Arba Minch University, Ethiopia

View Article Online
DOI: 10.1039/C5RA20576J

In this article fluorescence spectroscopy, UV-visible spectroscopy, circular dichroism (CD), isothermal titration calorimetry (ITC), transmission electron microscopy (TEM) and molecular docking methods have been used to examine the interaction between dicationic ester-bonded gemini surfactants (*m*-E2-*m*) and hen egg white lysozyme (HEWL). The fluorescence and UV measurements indicate *m*-E2-*m*-HEWL complex formation via static procedure. Binding isotherms reveal mainly cooperative binding of *m*-E2-*m* surfactants to HEWL. Circular dichroism, and pyrene fluorescence depict conformational changes in HEWL upon *m*-E2-*m* combination. Synchronous fluorescence shows that addition of *m*-E2-*m* has a remarkable effect on the polarity of the microenvironment in HEWL. Far-UV CD spectra demonstrate that the α-helical network of HEWL is disrupted and its content decreases from 30.68 % to 20.83%/20.40%, respectively, upon 12-E2-12/14-E2-14 combination. ITC confirms the endothermicity of *m*-E2-*m*-HEWL interactions while slight exothermicity was observed in the 14-E2-14-HEWL system at higher molar ratios of surfactant. TEM micrographs reveal structural change in HEWL upon *m*-E2-*m* addition. Molecular docking illustrates that 14-E2-14 binds principally to predominant fluorophores of lysozyme viz. Trp-108 and Trp-62 while 12-E2-12 binds in proximity of Trp-123. This study provides an important insight, particularly the contribution of Trp-123 in the fluorescence besides already known predominant fluorophores, Trp-62 and Trp-108. Moreover, this study would be significant in context of protein-surfactant interactions in terms of special *m*-E2-*m* molecular structure, which is essential in determining their future use as excipients in pharmaceutical/drug delivery related compilations.

View Article Online
DOI: 10.1039/C5RA20576J

1. Introduction

Owing to diverse implications in cosmetic, industrial, biological, and pharmaceutical compilations, [1-8] surfactants have been extensively studied from past few decades. Now-a-days, better-quality and second generation surfactants, gemini surfactants, are of great interest owing to their superior and outstanding properties than single tail/single head conventional surfactants. Compared to conventional surfactants, gemini surfactants dispatch outstanding properties viz., lower critical micelle concentration (CMC), better wetting, foaming and dispersing properties. Gemini surfactants also offer promising applications in prime research domains like gene transfection,[9] gene delivery[10] and compilation of antimicrobial, skin/body care and drug entrapment/delivery products.[11,12] Despite possessing properties of much interest for their possible end-use, cationic gemini surfactants are found toxic and responsible for skin irritation, eye infection, and related phenomenon.[13-15] Therefore, much efforts are being made to develop/design attractive featured, easily cleavable, biodegradable, environment friendly and low toxic ester-bonded surfactants (such as *m*-E2-*m*, where m is the tail chain length). The significance with ester functionalized surfactants is that they are easily cleavable and biodegradable under variant environmental conditions (like pH change, etc[16]).

Herein, the chosen *m*-E2-*m* surfactants are ester-functionalized with a diester linkage (E2) in the spacer part. This special structural feature enables them with lower CMC, biodegradability and lower toxicity properties. Moreover, presence of E2 moiety (being hydrophilic) enhances their self-aggregation capacity in polar and non-polar solvents via hydrogen bonding. Therefore, *m*-E2-*m* surfactants are pertinent and appropriate for study.

View Article Online
DOI: 10.1039/C5RA20576J

Hen egg white lysozyme (HEWL) is a small globular, monomeric protein with 129 amino acid residues in which the six tryptophan (Trp) residues are located as: substrate binding residues (3 Trp), hydrophobic core residues (2 Trp) and one Trp is separate from all other residues. The dominant fluorophores contributing to fluorescence are Trp-62 and Trp-108 and these are supposed to be important in binding a substrate or inhibitor and in stabilizing the structure. Motivation to choose HEWL for the study lies in the fact that it is being generally used as model system to understand the structure, function, dynamics and folding of proteins.[17] Moreover, lysozyme is known to posses various physiological and pharmaceutical (antivirus, antibacterial and antitumor) properties and have a versatile aptitude to interact with metal ions, drugs, dyes and surfactants.[18, 19]

Protein-surfactant interactions are pertinent and interesting not only for structural determination/protein separation, but because of their utilization in foods, cosmetics, drug delivery and other industrial applications.[20-22] Surfactants' structural features (spacer type/hydrophobic content) primarily control these interactions.[23] Further, these interactions are essential to explore surfactants as denaturants, solubilizing, and denaturizing agents for proteins.[1,2] Binding interaction of surfactants with proteins changes the conformation of the latter, therefore, it is essential to understand protein-surfactant interactions for scientific as well as practical view points. In addition, it has vast perspective to understand the role of surfactants in diseases such as amyloidosis.[24] Amyloidosis or fibril formation is associated and responsible for various diseases including Alzheimer's and Parkinson's diseases.[25] Several recent reports have revealed disintegration/modulation of BSA fibrils in presence of gemini surfactants.[25, 26] Therefore, we assume this study will have relevance to address the problems associated with protein misfolding in future. Also, it is reported that cationic gemini surfactants favour fibril

View Article Online
DOI: 10.1039/C5RA20576J

formation below the CMC and that the surfactants above their CMC can delay amyloid beta fibril formation.[21] Therefore, we expect *m*-E2-*m* would be good fibril modulators owing to their very low CMC values (about 100 times less than the conventional surfactants).

A large number of papers deal with the interaction of proteins with conventional surfactants (like SDS, CTAB and Triton-X-100[1,2,27-28]), but reports related to interaction of proteins with gemini surfactants are limited. Recent comparative reports on surfactant – protein interactions have demonstrated better efficacy of the gemini surfactants.[29-38] To the best of our knowledge, no report relating to interactions of *m*-E2-*m* and HEWL is available in the literature till date. Moreover, our previous studies have shown the effect of *m*-E2-*m* surfactants on globular xanthine oxidase (XO).[39-41] Therefore, in continuation of our previous studies and also keeping in interest the pharmaceutical, biotechnological and cosmetic relevance, herein, we have investigated the effect of *m*-E2-*m* novel biodegradable gemini surfactants on the structural features of HEWL by employing spectroscopic, calorimetric, microscopic and molecular docking approach. Fluorescence, CD, UV and ITC measurements were employed to investigate the binding mechanism, number of binding sites, binding forces, and conformational changes while computational docking was utilized to confirm the main binding site in HEWL. The results obtained in this study are quite encouraging and this study would be significant to protein-surfactant interaction in terms of special *m*-E2-*m* molecular structure, which is essential in determining their future use as excipients in membrane mimitics, pharmaceutical/drug delivery related compilations etc. Moreover, who could not be optimistic in future to construct surfactant based systems to disassemble amyloid fibrils into soluble substances.

View Article Online
DOI: 10.1039/C5RA20576J

2. Experimental

2.1 Materials

Chloroacetyl chloride (98%, Loba-Chemie, India), ethylene glycol (99%, Sigma Aldrich, USA), *N,N*-dimethyldodecylamine (95%, Sigma Aldrich, USA), *N,N*-dimethyltetradecylamine (95%, Sigma Aldrich, USA), hen egg white lysozyme (HEWL, Sigma Aldrich, USA), and pyrene (98%, Acros Organics, Belgium) were used as received. The gemini surfactants, ethane-1, 2-diyl bis (*N,N*-dimethyl-*N*-alkyl-ammoniumacetoxy) dichloride (*m*-E2-*m*; where *m* = number of carbon atoms in the tail and E2 represents diester spacer), were synthesized following the literature procedure[39-41] The synthesis protocol and structure of gemini surfactants are shown in Scheme 1 and Scheme 2. Working solution concentrations were: [HEWL] = 20×10^{-6} M, [PBS] = 12×10^{-3} M, pH= 7.4.

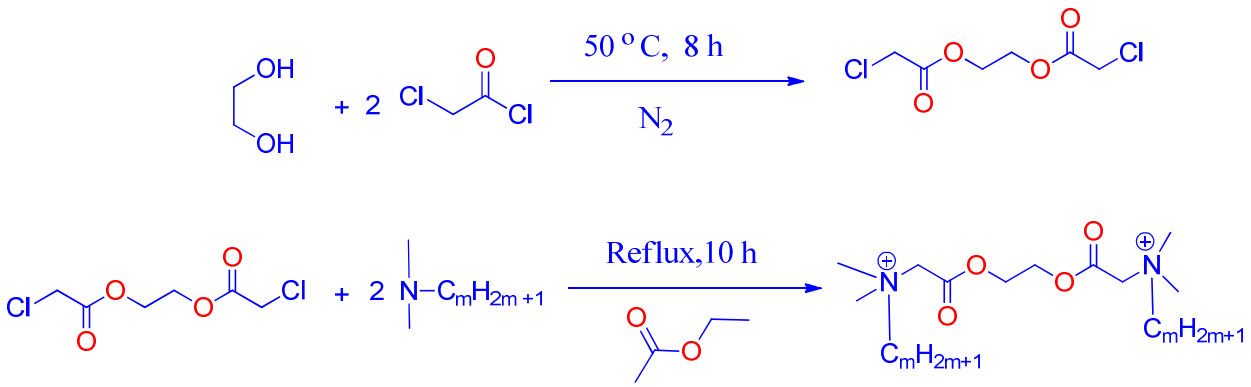

Scheme 1 Synthesis protocol of *m*-E2-*m* gemini surfactants (m=12, 14, is the number of carbon atoms in the tail of surfactant).

View Article Online
DOI: 10.1039/C5RA20576J

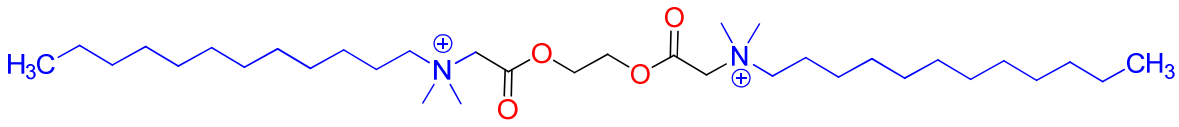

(a)

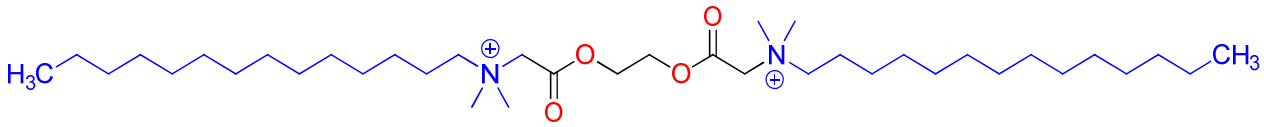

(b)

Scheme 2 Structures of *m*-E2-*m* gemini surfactants; (a) 12-E2-12 and (b) 14-E2-14.

2.2 Methods

2.2.1 Fluorescence measurements. The intrinsic fluorescence measurements were carried out using a Hitachi-2700 fluorescence spectrophotometer (Japan). The intrinsic fluorescence of HEWL was monitored at excitation wavelength of 280 nm and the emission spectra were recorded in the range of 300–450 nm. Both the slit widths (excitation as well as emission) were set at 5 nm. Synchronous fluorescence spectra of HEWL were recorded using the same spectrophotometer at a wavelength interval ($\Delta\lambda$) of 20 and 60 nm to probe, respectively, the microenvironment changes around the tyrosine (Tyr) and tryptophan (Trp) residues[42-44]. Three-dimensional fluorescence spectra were recorded in the range of 200 to 800 nm. For extrinsic pyrene fluorescence, the excitation was kept at 237 nm and emission was observed in the range of 350-450 nm.

View Article Online
DOI: 10.1039/C5RA20576J

2.2.2 UV measurements. The absorption spectra were recorded on Perkin Elmer Lambda-25 spectrophotometer in the wavelength range of 200-345 nm. The concentration of *m*-E2-*m* gemini surfactants were varied keeping HEWL concentration constant (20 μM).

2.2.3 CD measurements. Circular dichroism measurements were performed on JASCO-J815 CD spectropolarimeter equipped with a micro-computer. Prior to an experiment the instrument was calibrated with d-10 camphorsulfonic acid and parameters were set as: temperature, 298 K; average number of scans, 3; scan speed, 100 nm/min; scan range, 200-250 nm; and response time, 1s. Requisite solutions of HEWL and HEWL + m-E2-m (12-E2-12, 14-E2-14) were taken in a 0.1 cm path length cell and then the far-UV CD spectra were recorded. A reference signal of *m*-E2-*m* + buffer was subtracted from the CD signal for all measurements.

2.2.4 ITC measurements. The calorimetric measurements were performed with a MicroCal ITC-200 (USA) at 298 K. The sample cell was loaded with solution of HEWL (20 μM), and the titrant syringe was filled with 40 μL of *m*-E2-*m* solution and 2 μL of the solution was injected into the sample cell.

2.2.5 Molecular docking analysis. Computational molecular modeling was performed using molecular graphics program Hex 6.1.[45] The essential requirements were made available as: HEWL PDB (1 DPX, http://www.rcsb.org./pdb), mol files of *m*-E2-*m* (CHEMSKETCH, http://www.acdlabs.com), PDB files of *m*-E2-*m* (Chimera 1.9, www.cgl.ucsf.edu/chimera) and the final visual scenes of docked structures were observed utilizing graphics program, Pymol[46] (http://pymol.sourceforge.net). The docking experiment was run on computer with Windows 7 as an operating system.

2.2.6 Transmission electron microscopy (TEM) measurements. Transmission electron microscopy was performed on JEM-2100 (JEOL, Japan) electron microscope. Negative staining

View Article Online
DOI: 10.1039/C5RA20576J

method was used to prepare the HEWL and HEWL+ *m*-E2-*m* systems. Then TEM micrographs were taken after proper drying of samples in air for 1 day.

3. Results and discussion

3.1 HEWL–*m*-E2-*m* complex formation

In proteins, fluorescence emission of intrinsic fluorophores (tryptophan (Trp), tyrosine (Tyr) and phenylalanine (Phe)) are usually used to probe ligand-protein binding, protein conformation and intermolecular interactions.[39, 47] In case of HEWL fluorescence, emission is mainly due to Trp-108 and Trp-62. The crystal structure of HEWL delineates that these dominant fluorophores are located near the substrate binding site and are essential in HEWL structure stabilization and ligand-induced conformational change around binding site.[47] HEWL-surfactant interactions can be well investigated by exciting aromatic residues at wavelength 280 nm, as both residues (Tyr/Trp) are known to get excited at this particular wavelength.

The fluorescence emission spectra of HEWL in the absence and presence of *m*-E2-*m* gemini surfactants are shown in Fig.1. It can be seen that, with increasing surfactant concentrations, a decrease in fluorescence, accompanied by slight blue shift, is observed. This decrease in fluorescence intensity infers the non-fluorescent complex formation between HEWL and *m*-E2-*m* gemini surfactants. The small blue shift observed can be attributed to unfolding of HEWL upon *m*-E2-*m* addition.[35] It is also evident from Fig. 1 that 14-E2-14 causes larger diminution in fluorescence intensity than 12-E2-12, this being due to the higher hydrophobicity of the former. At pH 7.4, HEWL bears a net negative charge and offers well accountability to interact with the positively charged head groups of *m*-E2-*m* surfactants. As a result, *m*-E2-*m* aggregation on the protein surface increases, favoring the hydrophobic interactions; thus diminution with higher

View Article Online
DOI: 10.1039/C5RA20576J

chain length surfactant is justified. Similar results on fluorescence intensity of BSA were observed by Ge et al.[38] Moreover, Martin et al. also attributed higher quenching in BSA to a higher hydrophobicity exerted by the dimeric surfactants than the conventional one.[37] Thus, our results fit well to the recent literature reports.

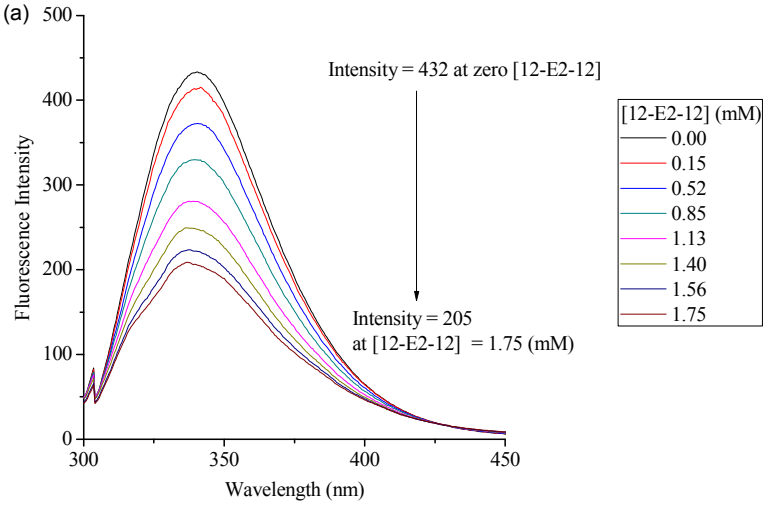

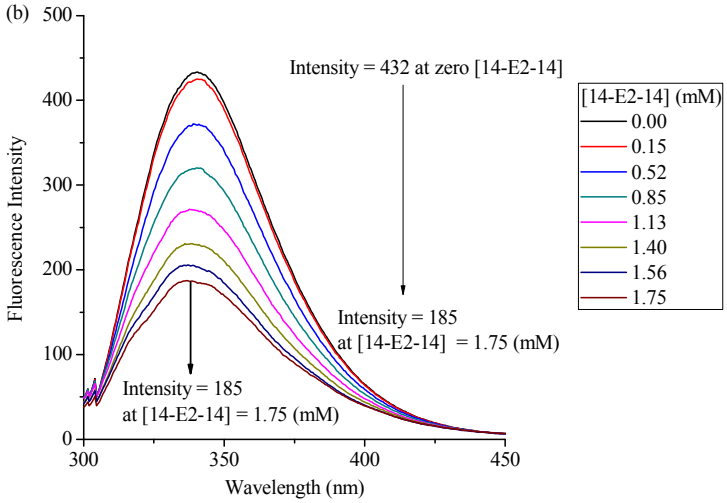

View Article Online
DOI: 10.1039/C5RA20576J

Fig. 1 Fluorescence emission spectra of HEWL in the absence and presence of 12-E2-12 (a), and 14-E2-14 (b) gemini surfactants at 298K and pH 7.4.

3.2 Binding mechanism, binding parameters, and binding isotherm

As is evident from Fig. 1, binding of *m*-E2-*m* gemini surfactants quenches the fluorescence intensity of HEWL. This quenching of fluorescence intensity may be static or dynamic. To confirm the exact quenching mechanism, the fluorescence data were analyzed by Stern-Volmer equation (1) [48]

$$\frac{F_0}{F} = 1 + K_{SV}[m\text{-}E2\text{-}m] \qquad (1)$$

where F_0 and F are the fluorescence intensities of HEWL in the absence and presence of the quencher, K_{sv} is the Stern−Volmer quenching constant (which reflects the extent of quenching), and [*m*-E2-*m*] is the concentration of the quencher. Fig. 2 gives the Stern−Volmer plots of HEWL−*m*-E2-*m* systems whose slopes were used to calculate the Stern-Volmer constant.

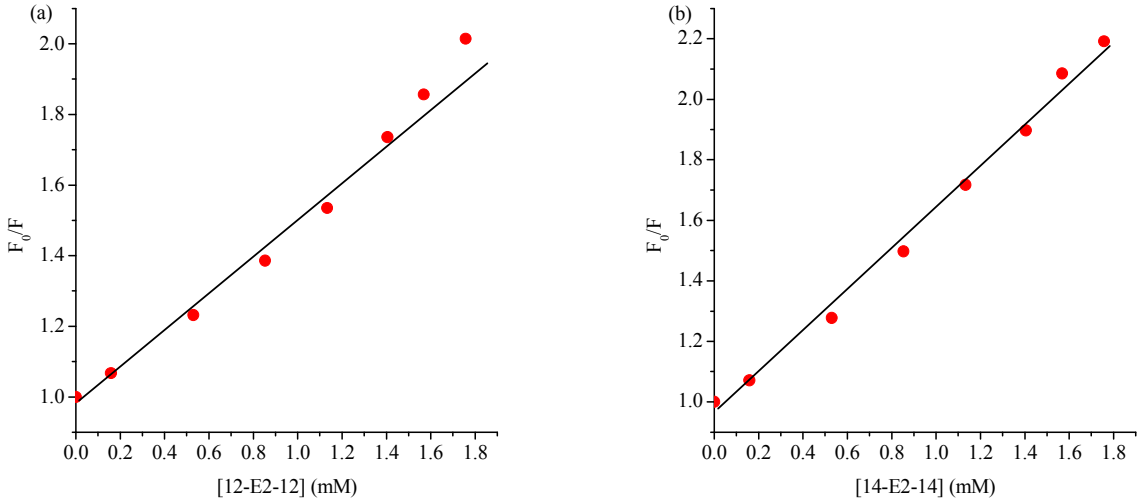

View Article Online
DOI: 10.1039/C5RA20576J

Fig. 2 Stern–Volmer plots of fluorescence quenching of HEWL by 12–E2-12 (a), and 14-E2-14 (b) gemini surfactants.

Significant K_{sv} values (Table 1) indicate substantial quenching of fluorescence spectra by the *m*-E2-*m* surfactants. These K_{sv} values were then used to evaluate bimolecular quenching rate constants (k_q) from equation (2)

$$k_q = \frac{K_{SV}}{\tau_0} \quad (2)$$

(τ_0 being the average lifetime of the fluorophore in the absence of quencher with a value of 10^{-8} s for most of the biomolecules).[49,50] It can be observed from the Table 1 that 14-E2-14 has higher value of quenching rate constant than 12-E2-12, indicating higher quenching efficiency of 14-E2-14 than 12-E2-12. Further, quenching rate constant was found two orders of magnitude than the scattering collision quenching rate constant (2×10^{10} L mol^{-1} s^{-1})[49], suggesting that the mechanism of quenching proceeds through static procedure and, therefore, is assumed to initiate via ground state complex formation between *m*-E2-*m* and HEWL.[49]

To obtain binding parameters, the fluorescence data were further analyzed by equation (3)

$$\log \{(F_0 - F)/F\} = \log K_b + n \log [m - E2 - m] \quad (3)$$

where F_0 and F are the same as in eq.(1), K_b and n represent the binding constant and number of binding sites, respectively, and are obtainable from the intercept and slope of $\log\{(F_o-F)/F\}$ versus log[*m*-E2-*m*] plots (Fig. 3). The obtained K_b and n values are given in Table 1.

View Article Online
DOI: 10.1039/C5RA20576J

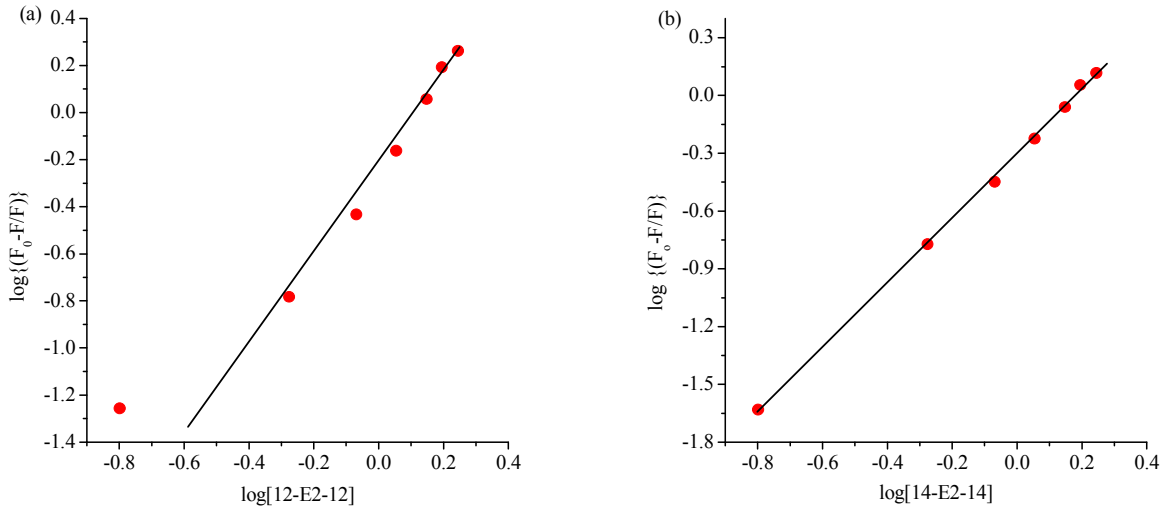

Fig. 3 Plots of log {(F_0-F)/F} versus log [*m*-E2-*m*] at 298K and pH 7.4.

A higher K_b value of 14-E2-14 depicts that it binds more effectively than 12-E2-12. Further, the values of n, found to be 1.35 and 1.67, respectively, for 12-E2-12 and 14-E2-14, confirm single pattern of binding sites on HEWL for the *m*-E2-*m* gemini surfactants.

Table 1 Binding parameters for the interaction of *m*-E2-*m* surfactants with HEWL at pH 7.4 and 298K

System	K_{SV} (M^{-1})	k_q (L mol^{-1} s^{-1})	R^2	K_b (M^{-1})	R^2	ΔG_b° (kJ mol^{-1})	n
12-E2-12+HEWL	5.3×10^4	5.3×10^{12}	0.98	4.5×10^4	0.99	–26.55	1.35
14-E2-14+HEWL	6.5×10^4	6.5×10^{12}	0.98	4.9×10^4	0.99	–26.76	1.67

View Article Online
DOI: 10.1039/C5RA20576J

The average number of *m*-E2-*m* surfactant molecules (υ), bound to HEWL, were also computed by using the following equation

$$\upsilon = \alpha\,(C_{m\text{-E2-}m}/C_{\text{HEWL}}) \quad (4)$$

where C represents the molar surfactant concentration of the indicated species. α (the fraction of *m*-E2-*m* molecules bound to HEWL) was estimated from equation (5)[29]

$$\alpha = \frac{F_{obs} - F_o}{F_{min} - F_o} \quad (5)$$

where F_{obs} is the HEWL fluorescence intensity at any surfactant concentration, F_o is the HEWL fluorescence intensity in the absence of surfactant, and F_{min} is the minimal HEWL fluorescence intensity observed in the presence of surfactant. It is clearly seen (Fig. 4) that there are two regions of binding in the chosen concentration range of the surfactants. The first region (lower sloppy region), at lower concentrations of *m*-E2-*m* gemini surfactants, corresponds to non-cooperative binding, and the second region reveals abrupt increase in binding, which can be attributed to cooperative binding of *m*-E2-*m* surfactants to HEWL. Thus, from the binding isotherms, we can conclude that binding of *m*-E2-*m* surfactants is mainly governed by cooperative interactions. The reason for these cooperative interactions can be attributed to the higher aggregation of *m*-E2-*m* microstructures at higher surfactant concentrations.

View Article Online
DOI: 10.1039/C5RA20576J

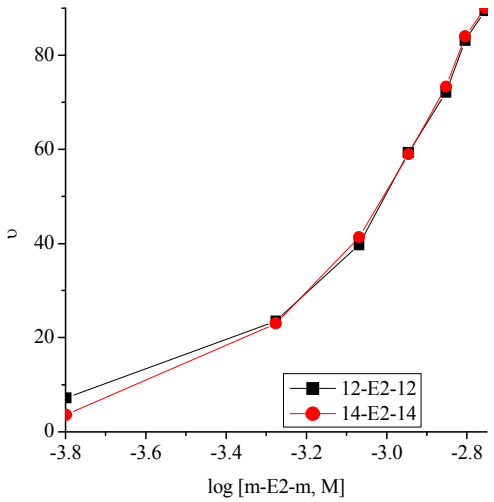

Fig. 4 The binding curves of the *m*-E2-*m* gemini surfactants with HEWL at pH 7.4 and 298 K.

3.3 Three-dimensional fluorescence spectroscopy

Three-dimensional fluorescence spectroscopy is an essential analytical technique to comprehensively exhibit the fluorescence information and conformational changes of proteins in a more suitable and realistic way.[51] Fig. 5 shows the three-dimensional fluorescence spectra of HEWL in the absence and presence of *m*-E2-*m* surfactants. Two peaks are seen in the spectra; peak 1 is the Rayleigh scattering peak and peak 2 reveals the behaviour of aromatic residues (Tyr/Trp) and is correlated to the micropolarity around these residues. The fluorescence intensity of peak 2 decreases in the presence of *m*-E2-*m* surfactants, suggesting that micropolarity of these residues changes (Fig. 5b and Fig. 5c) due to the exposure of aromatic residues to an outer environment. Moreover, this quenching of peak 2 is also attributed to the formation of HEWL-*m*-E2-*m* complex formation. Thus, the results are consistent with the above mentioned techniques.

View Article Online
DOI: 10.1039/C5RA20576J

(a)

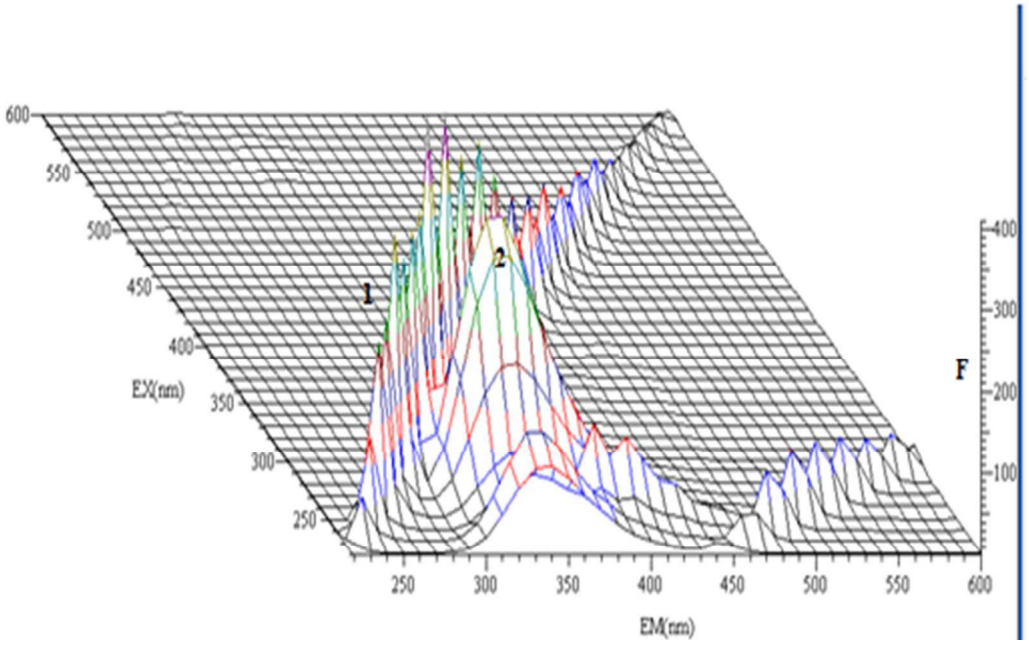

(b)

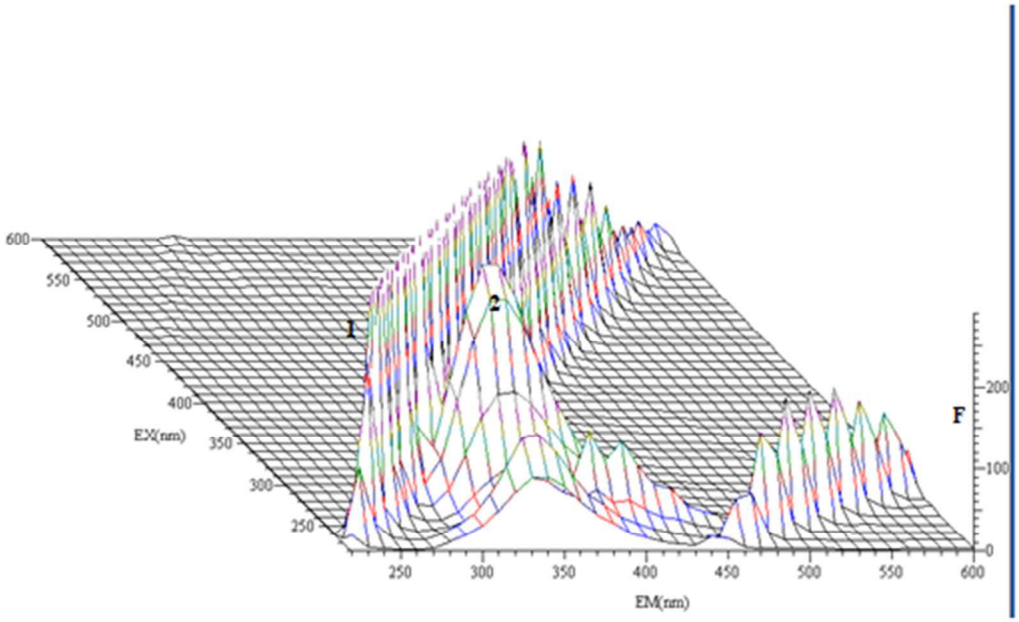

View Article Online
DOI: 10.1039/C5RA20576J

(c)

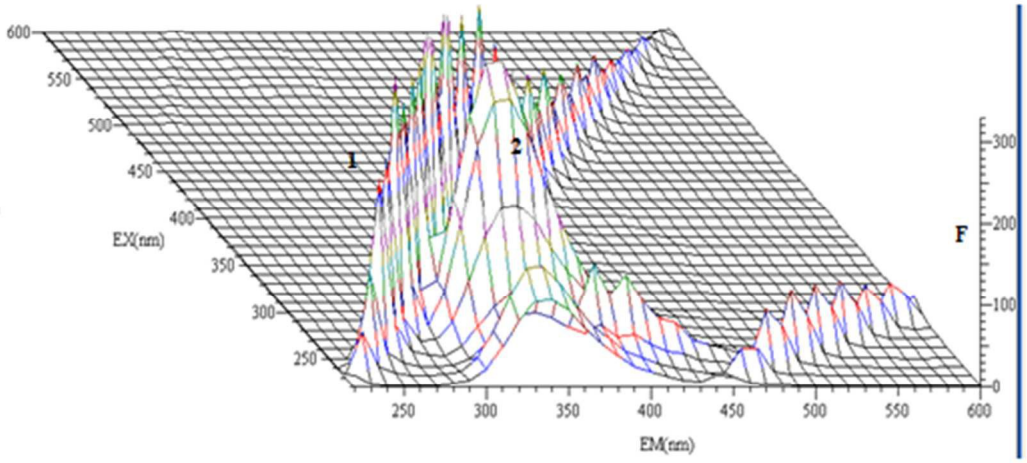

Fig. 5 Three-dimensional fluorescence spectra of native HEWL (a), HEWL + 12-E2-12 (b), and HEWL + 14-E2-14 (c) at 298K and pH 7.4; [HEWL] = 20 μM, [12-E2-12] and [14-E2-14] = 1.13mM.

3.4 Synchronous fluorescence spectroscopy

For obtaining specific micropolarity information around the tyrosine (Tyr) and tryptophan (Trp) residues, synchronous fluorescence spectroscopy is considered an appropriate technique.[52, 53] Its specialty is also owing to its important features such as spectral bandwidth reduction, spectral simplification and avoiding different perturbing effects. Fig. 6 shows the synchronous fluorescence spectra of HEWL in the absence and presence of *m*-E2-*m* surfactants. Quite interestingly, it can be seen from the synchronous spectra that subsequent additions of *m*-E2-*m* quenches the fluorescence intensity around both the residues, indicating the binding of *m*-E2-*m* gemini surfactants to HEWL. The non-polar environment generated by the *m*-E2-*m* gemini surfactant around aromatic residues can be accountable for the same. It is also evident that the

View Article Online
DOI: 10.1039/C5RA20576J

Trp residues contribute more to the intrinsic fluorescence of HEWL than the Tyr residues, because the fluorescence intensity at 60 nm is higher than that at 20 nm (Fig. 6b and Fig. 6d)). A comparative analysis of the spectra reveals that 14-E2-14 interacts strongly with both the residues than 12-E2-12; again higher hydrophobic contribution of the former are being attributable.

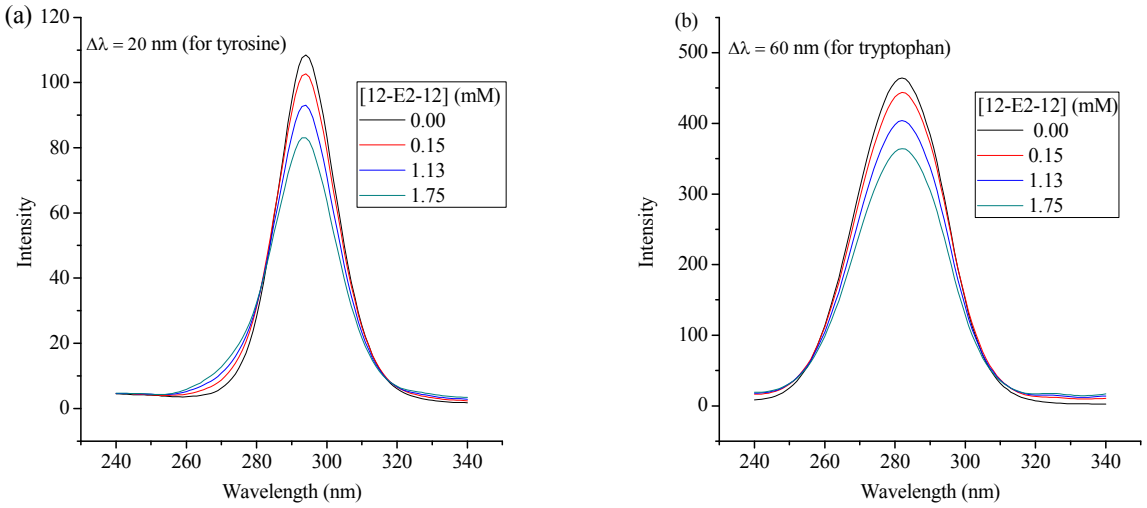

View Article Online
DOI: 10.1039/C5RA20576J

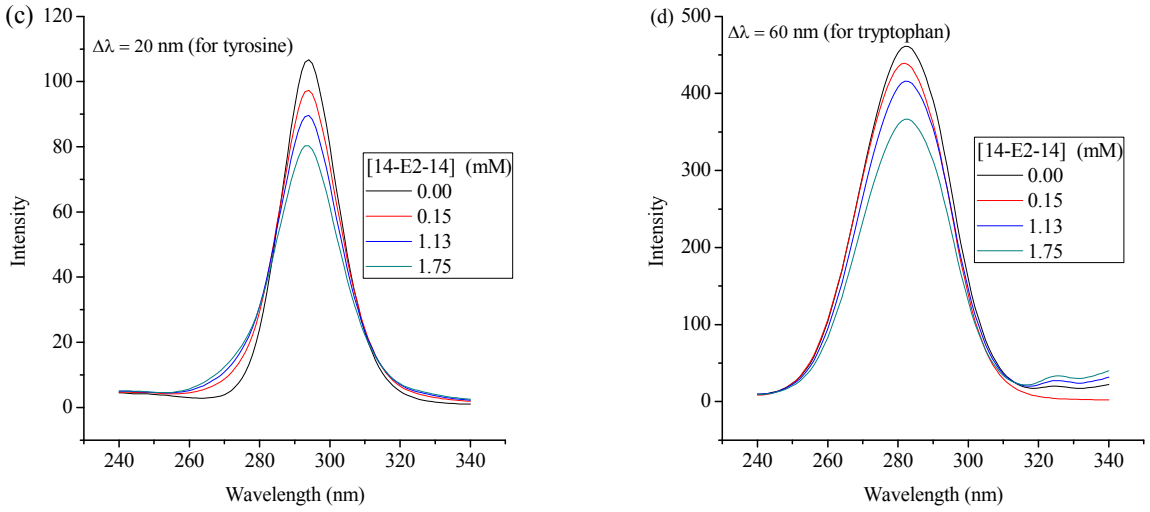

Fig. 6 Synchronous fluorescence spectra of HEWL in the absence and presence of various concentrations of *m*-E2-*m* gemini surfactants.

Moreover, the synchronous fluorescence spectroscopy was further employed to confirm the quenching mechanism[54]. The data were fitted in equation (6) and the obtained plots of reduction in synchronous fluorescence intensity with concentration of *m*-E2-*m* gemini surfactants are shown in Fig. 7.

$$\frac{F_0}{F} = 1 + (K_{SV} + k_q \tau_0)[m\text{-}E2\text{-}m] + K_{SV} k_q \tau_0 [m\text{-}E2\text{-}m]^2 \qquad (6)$$

It can be clearly seen that all plots are linear, devoid of upward curvature (which is possibly in both dynamic and static situations), inferring that complex formation proceeds through static quenching rather than dynamic one. Further, absence of upward curvature depicts the independency on the square part of equation (6).

View Article Online
DOI: 10.1039/C5RA20576J

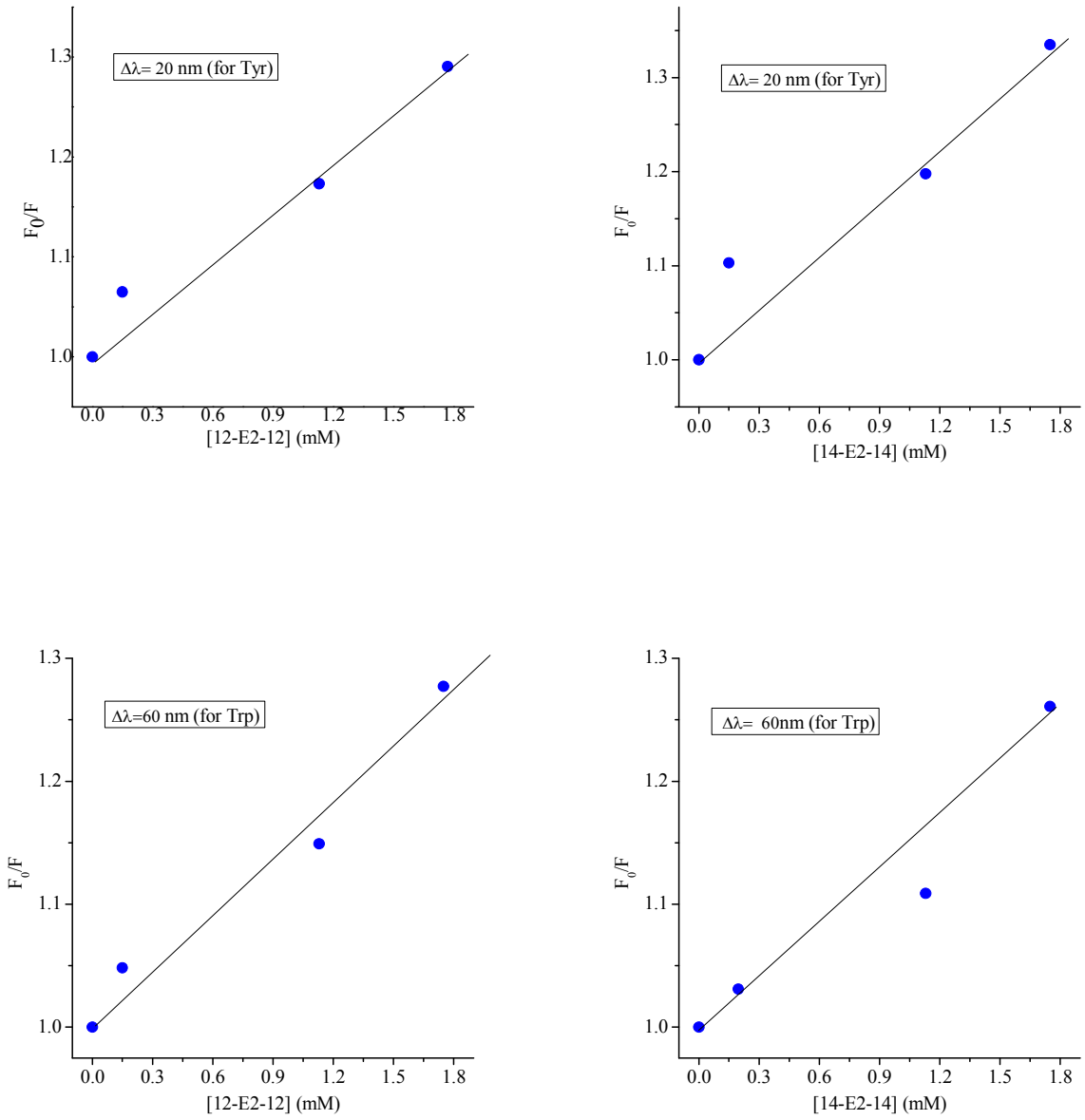

Fig. 7 Reduction in synchronous fluorescence intensity of HEWL by *m*-E2-*m* gemini surfactants at Δλ= 20 nm (for tyrosine) and Δλ = 60 nm (for tryptophan).

View Article Online
DOI: 10.1039/C5RA20576J

3.5 Micropolarity assay

In order to further investigate the micropolarity changes around the aromatic residues, pyrene fluorescence was used[55]. Pyrene serves as probe in *m*-E2-*m*–HEWL system and is sensitive to micropolarity changes. The five-peaked pyrene emission spectra of HEWL in the absence and presence of different concentrations of *m*-E2-*m* surfactants are shown Fig. 8. In the absence of surfactants, the fluorescence intensity is low, indicating that pyrene is localized in the Trp/Tyr residues. Additions of gemini surfactant increases the fluorescence intensity, which implies the exposure of aromatic residues. At higher concentrations of *m*-E2-*m*, on the other hand, decrease in fluorescence intensity is observed, most probably due to incorporation of probe molecules (pyrene) into the *m*-E2-*m* aggregates.

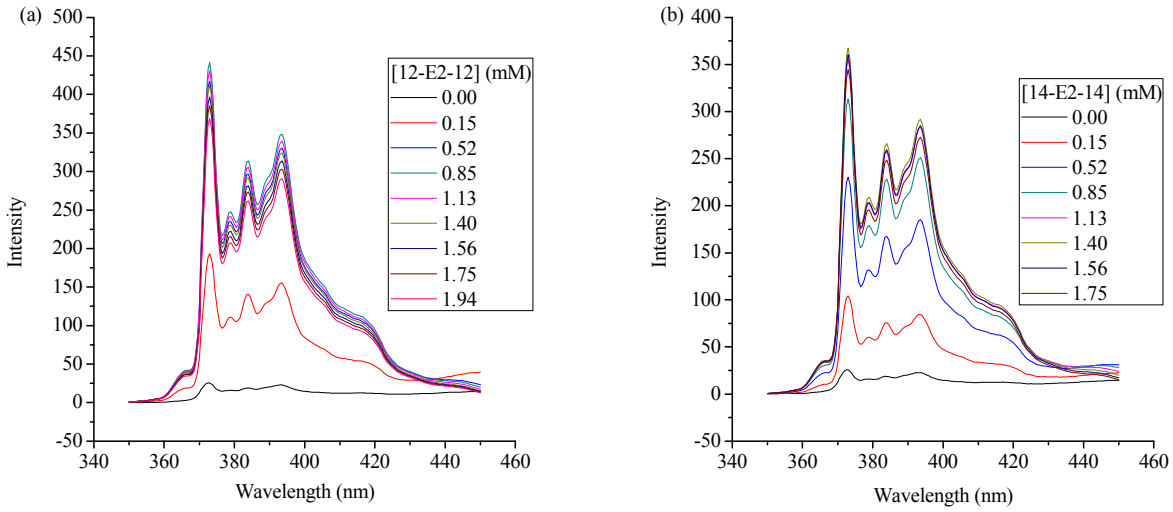

Fig. 8 Pyrene emission fluorescence spectra of HEWL in the absence and presence of varying concentrations of 12-E2-12 (a) and 14-E2-14 (b) at 298K and pH 7.4.

View Article Online
DOI: 10.1039/C5RA20576J

Moreover, the F_1/F_3 ratios, computed on the basis of first and third vibrational peaks[55] and depicted in Fig. 9, show that the ratio of native HEWL is low, indicating pyrene to be in the hydrophobic network. On subsequent additions of *m*-E2-*m* gemini surfactants, the ratio slightly increases, revealing its exposure to outer environment. Constancy and decrease at higher concentrations can be attributed to numerous aggregated structures formed by *m*-E2-*m* at higher concentrations. Lower F_1/F_3 ratios, observed for HEWL-14-E2-14 surfactant, indicate higher potential of 14-E2-14 to influence the microstructure of HEWL.

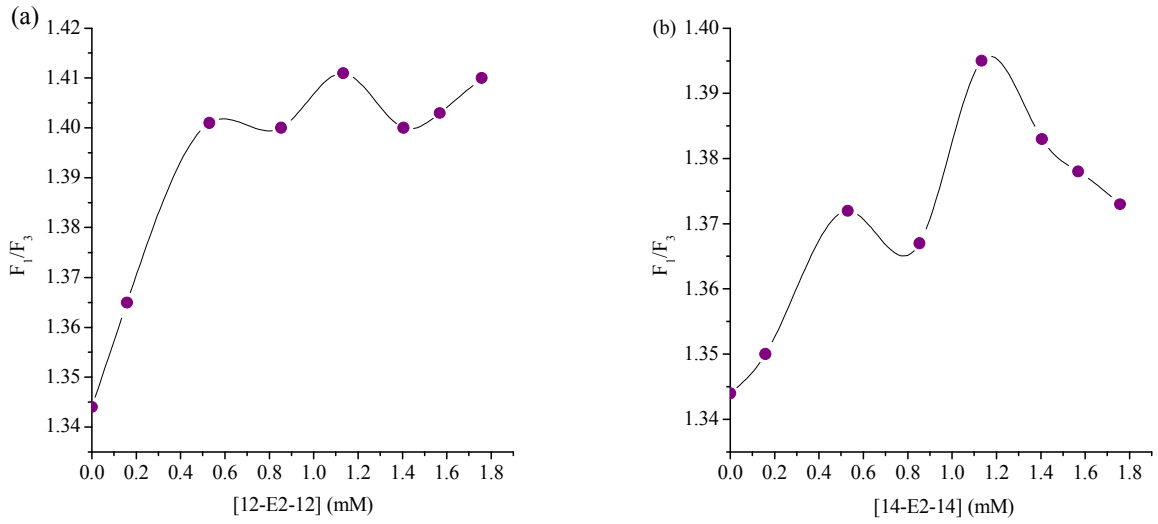

Fig. 9 Variation of F_1/F_3 ratio as a function of *m*-E2-*m* concentration.

3.6 UV-vis absorption spectroscopy

UV-Vis spectroscopy is extensively used to investigate structural changes of proteins and to explore ligand–protein complex formations. It is known as a straight-forward but efficient technique in detecting complex formation.[56,57] The UV-vis spectra of HEWL at different gemini

View Article Online
DOI: 10.1039/C5RA20576J

concentrations (Fig. 10) show maximum absorption band at 279 nm, related to electron transition (π–π^*) of π bonds of aromatic residues. The relevant spectra show hyposchromism/hypsochromism effects upon the addition of *m*-E2-*m* surfactants, signifying *m*-E2-*m*–HEWL complex formation and the observed small blue shift is indicative of unfolding of HEWL upon *m*-E2-*m* combination. The blue shift being more prominent in 14-E2-14-HEWL combination is due to the higher efficiency of 14-E2-14 towards HEWL (than 12-E2-12) to change the protein structure.

As explained in fluorescence spectroscopic results, the quenching mechanism is static; this is further supported by changes in the UV-visible spectrum of HEWL. As per literature, [58-60] in case a complex of protein and ligand is formed through static quenching, then there will be some changes in the UV-vis spectrum of the protein, whereas dynamic quenching produces no such change. In our case, the UV-vis spectra show substantial change upon gemini-surfactant combination; thus we can safely conclude that the quenching is primarily caused by complex formation between *m*-E2-*m* and HEWL. Obviously, our results are in mutual complement with the fluorescence results. Moreover, similar quenching validation by UV-vis spectra was also reported by another research group.[4]

View Article Online
DOI: 10.1039/C5RA20576J

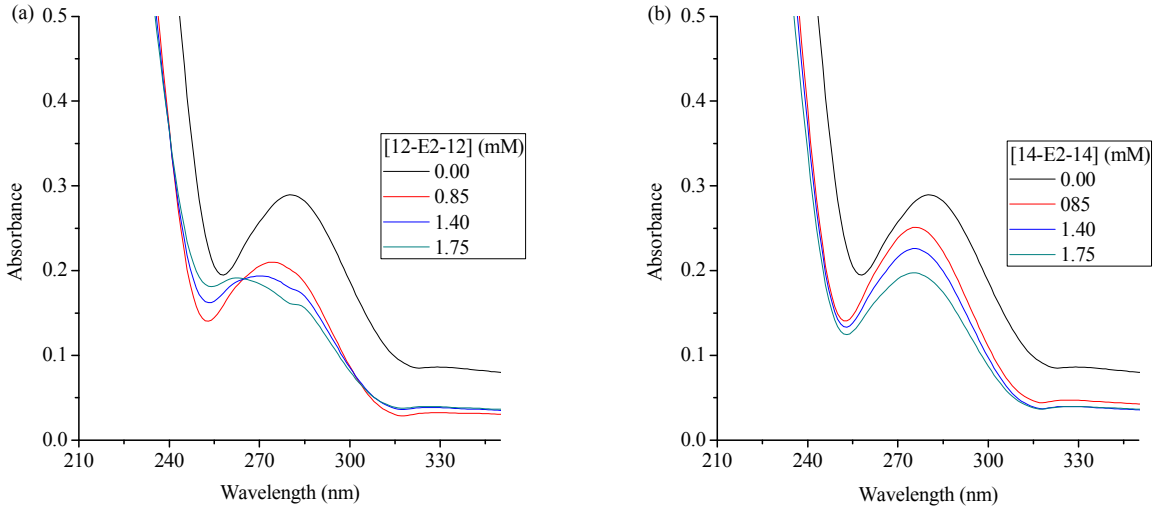

Fig. 10 UV spectra of HEWL in the absence and presence of 12-E2-12 (a) and 14-E2-14 (b) gemini surfactants.

Thus, by analyzing different spectroscopic techniques it is found that all the techniques are in well corroboration with each other. Intrinsic fluorescence spectroscopy depicts substantial binding of *m*-E2-*m* gemini surfactants to HEWL which, in three-dimensional fluorescence is indicated by distinct quenching at higher surfactant concentrations. In case of synchronous fluorescence spectroscopy, mixed systems are found to have lower fluorescence intensity than native HEWL which again is in well coherence with pyrene fluorescence in which we obtained lower F_1/F_3 ratios. Hypochromic/hypsochromic effects observed in UV-vis spectroscopy further advocate the microenvironmental change around aromatic residues of HEWL upon gemini combination.

View Article Online
DOI: 10.1039/C5RA20576J

3.7 Conformational analysis (circular dichroism spectroscopy)

The CD spectroscopy can be exploited to explore fluctuations in the secondary structure of proteins during binding process. The CD spectra of the native HEWL at different concentrations of *m*-E2-*m* gemini surfactants are shown in Fig. 11. Two negative bands are exhibited in the far-UV region at around 208 and 222 nm, which are characteristic of the α-helical structure and attributed to n-π* transitions.[61] Alterations in ellipticity at 208 nm are useful for visualizing variations in the α-helical content. Fig. 11 shows that the addition of surfactants results in a decrease of negative helicity, suggesting unfolding of HEWL.

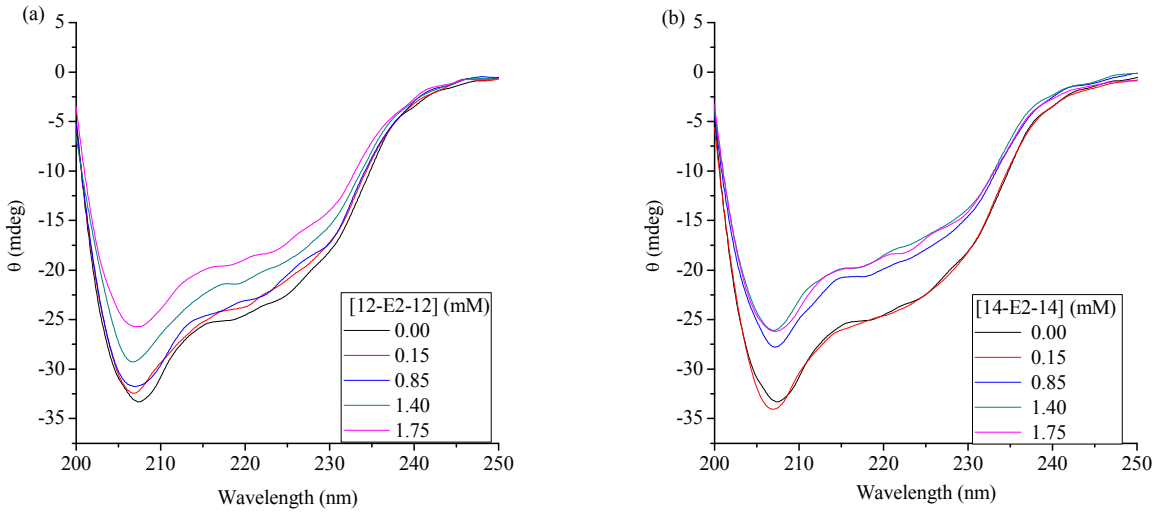

Fig. 11 Far-UV CD spectra of HEWL in the absence and presence of 12-E2-12 (a), and 14-E2-14 (b) gemini surfactants.

As per equation (7), the CD results are expressed in terms of mean residue ellipticity (MRE) in degree cm^2 $dmol^{-1}$

View Article Online
DOI: 10.1039/C5RA20576J

$$\mathrm{MRE} = \frac{\mathrm{Observed\,CD\,(m\,degree)}}{\mathrm{C_{HEWL}}\, n\, l \times 10} \tag{7}$$

where C_{HEWL} is the molar concentration of the protein, n is the number of amino acid residues (129), and l is the path length (0.1 cm). Then, using equation (8), the α-helical content

$$\alpha - \mathrm{Helix}\ (\%) = \frac{\mathrm{MRE}_{208} - 4000}{33{,}000 - 4000} \times 100 \tag{8}$$

of HEWL was evaluated. It can be seen (Table 2) that the α-helicity decreases, inferring that binding of *m*-E2-*m* to HEWL may induce some conformational changes.[65] The trend to decrease α-helicity among the geminis is 14-E2-14 > 12-E2-12. The reason might lie in the fact that more hydrophobic nature of 14-E2-14 causes more extended polypeptide structure of HEWL which leads to an exposure of the hydrophobic cavities and hence α-helical content decreases significantly.[62] It is also interesting to note that the obtained CD signals are of similar shape, indicating that the secondary structure (α-content) remains predominant even after binding of *m*-E2-*m* to the protein.[61]

Table 2 Variation of α-helical content of HEWL as function of *m*-E2-*m* (12-E2-12, 14-E2-14) gemini surfactant concentration

Gemini surfactant	Concentration of gemini surfactant (mM)	α–helical content (%)
12-E2-12	0	30.68
	0.15	29.96
	0.85	28.34
	1.40	25.11

View Article Online
DOI: 10.1039/C5RA20576J

	1.75	20.83
14-E2-14	0.15	31.84
	0.85	23.79
	1.40	21.14
	1.75	20.40

3.8 Isothermal titration calorimetry (ITC)

Isothermal titration calorimetry (ITC) is an essential technique to probe protein–ligand interactions. It directly measures the thermodynamic heat change of molecular interactions. The calorimetric profiles of binding of *m*-E2-*m* with the lysozyme are shown in Fig. 12. It can be seen that the titration curves lie mainly in the endothermic domain and show maximum endothermicity at very low *m*-E2-*m* concentration, followed by decrease in endothermicity. The endothermic contributions may be ascribed to hydrophobic forces governing complex formation with *m*-E2-*m*. Breaking of hydrogen bonding interactions due to cross linking of dimeric tails of *m*-E2-*m* geminis with amino acid residues of HEWL may also be responsible for positive enthalpy values. Interestingly, the behavior of 14-E2-14 is different (Fig. 12b) from 12-E2-12 . Its reaction profile first shows high endothermicity, which decreases to zero and crosses into the exothermic domain. The reasons for endothermicity are explained above, however, exothermicity can be ascribed to dominance of Van der Waals/ electrostatic interactions between the polar amino acid residues (like His, Arg, and Lys) of HEWL and the carbonyl group of the ester gemini surfactant.[63] Moreover, as the hydrophobic patches are located deeper,[64] it is easier for the shorter tail surfactant molecules to approach the residues and in order to generate the influence. A longer tail surfactant can generate more powerful hydrophobic interactions even by

View Article Online
DOI: 10.1039/C5RA20576J

residing at surface sites. In both cases, the hydrophobic forces remain predominant. However, when chain length is intermediate (like in 14-E2-14), chances of hydrophobic as well as electrostatic interactions are equally probable. This could be the other reason that at higher loadings of 14-E2-14, the endothermic event changes into exothermicity. Moreover, positive ΔH also suggests that the interaction must have proceeded with positive entropy (ΔS) change, necessary to cover the criteria of spontaneity of molecular reactions.

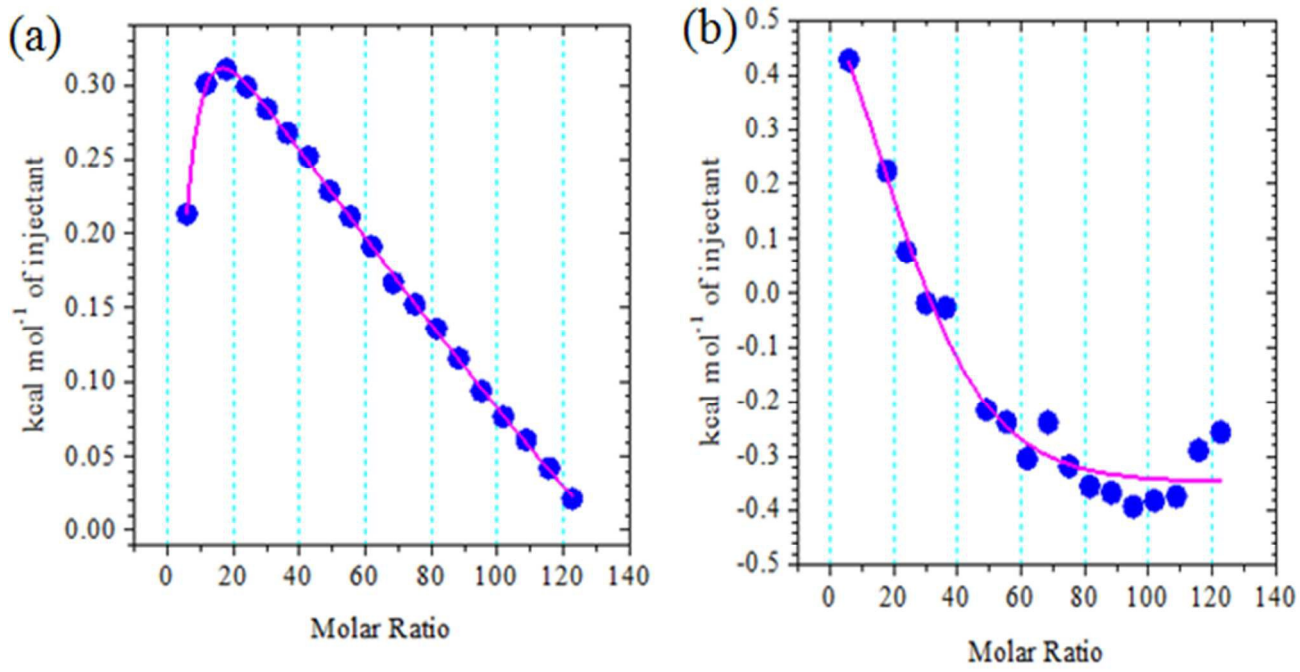

Fig. 12 Isothermal titration calorimetric curves of 12-E2-12 + HEWL (a), and 14-E2-14 + HEWL (b) systems at 298 K and pH 7.4.

Further, it can be interestingly noted (Table 3) that magnitude of binding parameters (K_b, ΔG_b°), obtained in ITC, are higher than the fluorescence binding parameters; the reason being ITC measures the global change (i.e. enthalpy change of the binding reaction as well as the enthalpy of all possible concomitant reactions which may accompany the binding reactions but

View Article Online
DOI: 10.1039/C5RA20576J

not directly influencing the K_b), while as fluorescence is specific to aromatic residues[65]. Moreover, n=2, which suggests the possibility of two binding sites, which is different from one binding site approximation of fluorescence. It may be due to absence of tryptophan residues in the close vicinity of binding event captured by fluorescence. Higher values of binding parameters obtained in ITC may also be ascribed to relatively longer twin tails of *m*-E2-*m* gemini surfactants, as it is known that longer chains (with 16-22 carbon atoms) can alter K_b values strongly[66].

Table 3 ITC derived biophysical parameters for the binding of *m*-E2-*m* surfactants with HEWL at at 298K and pH.7.4

System	K_b (M^{-1})	ΔH° (cal mol^{-1})	ΔS° (cal mol^{-1} K^{-1})	ΔG_b° (kcal mol^{-1})	n
12-E2-12-HEWL	5.63×10^{18}	181.7	86.4	–25.55	2
14-E2-14-HEWL	1.19×10^{19}	902.4	90.3	–26.00	2

3.9 Docking analysis of HEWL-*m*-E2-*m* complex

Molecular docking is considered an essential technique to unveil interactions between ligands and proteins[67]. It provides information about the binding site of ligand on protein, which has relevance in pharmaceutical science. In this context, we have performed a molecular docking of *m*-E2-*m* gemini surfactants with HEWL. The best-docked structures (with lower energy conformation) are shown in Fig. 13. Interestingly, we note that 12-E2-12 binds in the close proximity of Arg-128, Cys-6, Ala-122, Cys-33, Cys-30, Cys-116, Arg-112, Ala-107, Trp-108, Trp-63, Trp-62, Cys-64, Tyr-53, Asp-52, Trp-123, Val-123, Val-29, Phe-34 and Val-29, amino acid residues (Fig. 13a and Fig. 13b) while 14-E2-14 positions itself in the cavity lined by Val-

View Article Online
DOI: 10.1039/C5RA20576J

109, Val-99, Val-92, Tyr-53, Tyr-23, Ala-10,Trp-108, Ala-107, Trp-63, Trp-62, Arg-61, Ser-86, Thr-90, Asn-93, Ser-81 and Glu-35 residues (Fig. 13c and Fig.13d) . Moreover, the hydrophobic tail of 14-E2-14 lies in close vicinity of Tyr-62, Trp-63, Trp-108 aromatic residues and 12-E2-12 binds near Trp-123 site, suggesting that, besides the already known predominant fluorophores viz. Trp-62 and Trp-108, Trp-123 can also contribute to the fluorescence of HEWL. The presence of *m*-E2-*m* tail near the hydrophobic residues suggests the predominance of hydrophobic forces and, therefore, this observation lies in uniformity with the results obtained by fluorescence and ITC methods. Further, binding interaction energies for 12-E2-12 + HEWL and 14-E2-14 + HEWL are found to be –276.43 kJ mol^{-1} and –319.86 kJ mol^{-1}, respectively. This means that 14-E2-14 interacts strongly than 12-E2-12. The negative sign of binding interaction energies confirms that binding of *m*-E2-*m* to HEWL is spontaneous and thus supports our fluorescence results. Besides the above discussed interactions, possibility of hydrogen bonding interactions between carbonyl oxygen (C=O) of surfactant and nitrogen (N) of Asn and Arg-like residues cannot be ruled out. Hydrogen bonding interactions decrease the hydrophilicity and increase hydrophobicity, therefore, increase the overall stability of *m*-E2-*m*–HEWL complex. The values of interaction free energies obtained in molecular docking are not comparable to fluorescence results; the reason could be the exclusion of solvent in docking simulations or the X-ray structure of protein from crystals differs from the protein obtained in aqueous system.[50]

View Article Online
DOI: 10.1039/C5RA20576J

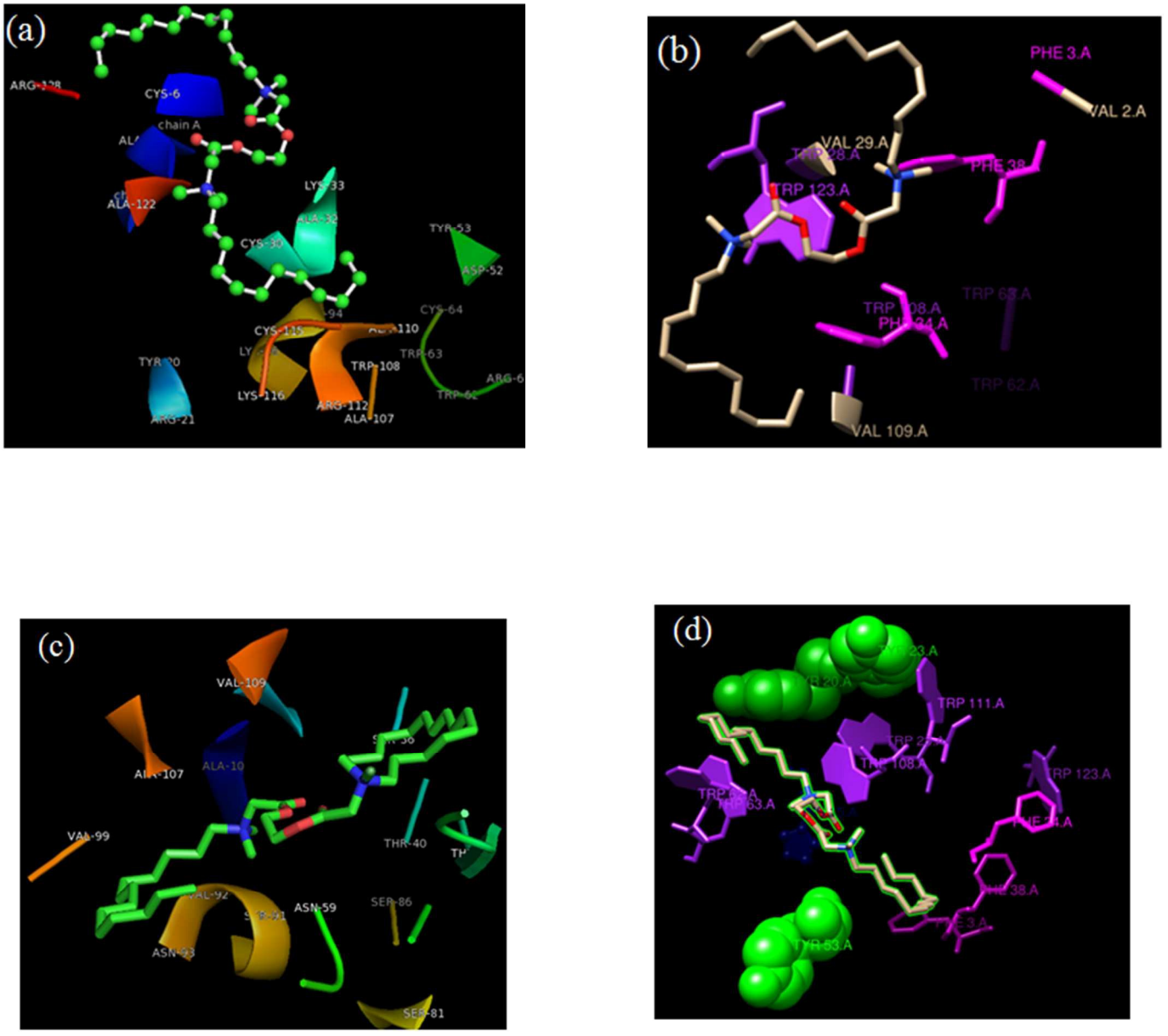

Fig. 13 Docked pose of HEWL with *m*-E2-*m* gemini surfactants: (a) HEWL + 12-E2-12 (PyMol view), (b) HEWL + 12-E2-12 (Chimera view), (c) HEWL + 14-E2-14 (PyMol view), and (d) HEWL + 14-E2-14 (Chimera view).

View Article Online
DOI: 10.1039/C5RA20576J

3.10 Microscopic TEM analysis

To further authenticate that the addition of *m*-E2-*m* surfactants results in structural change in the HEWL, we have performed transmission electron microscopy (TEM). TEM micrographs were obtained for native HEWL and mixed HEWL+ *m*-E2-*m* systems (Fig. 14). It can be seen that the mixed systems (Fig 14b and Fig. 14c) show aggregated structures rather than the native HEWL (Fig.14a), suggesting conformational change in HEWL upon gemini combination. Comparatively, larger aggregated structures are apparent in 14-E2-14 + HEWL than in 12-E2-12+ HEWL systems; the reason being the higher efficacy of 14-E2-14 to alter the enzyme structure. Hydrophobic as well as electrostatic interactions may be attributive. At higher concentration of surfactant, 14-E2-14 micelles adsorb at the HEWL backbone and generate repulsions among the head groups which destabilize the enzyme structure and induce aggregation. Moreover, in our ITC results (for 14-E2-14 + HEWL), we have also observed exothermicity at higher concentrations of 14-E2-14, which also supports the dominance of electrostatic interactions. Thus, both the techniques provide consistent results. Moreover, on the whole our overall results get further support from similar studies by Zhao et al [68-72].

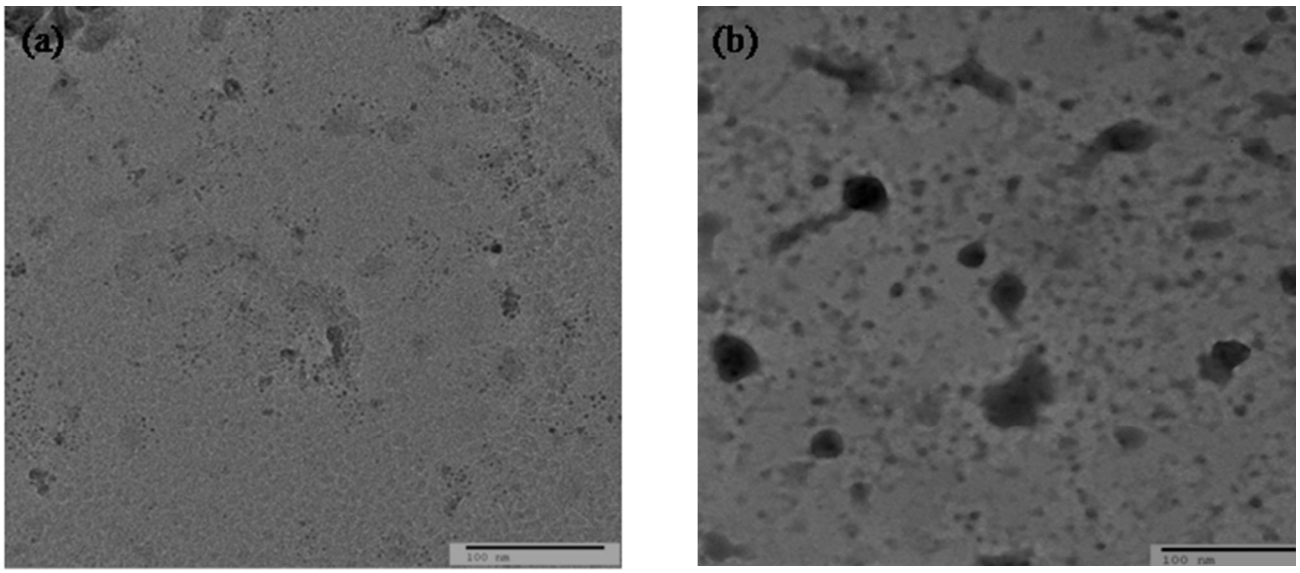

View Article Online
DOI: 10.1039/C5RA20576J

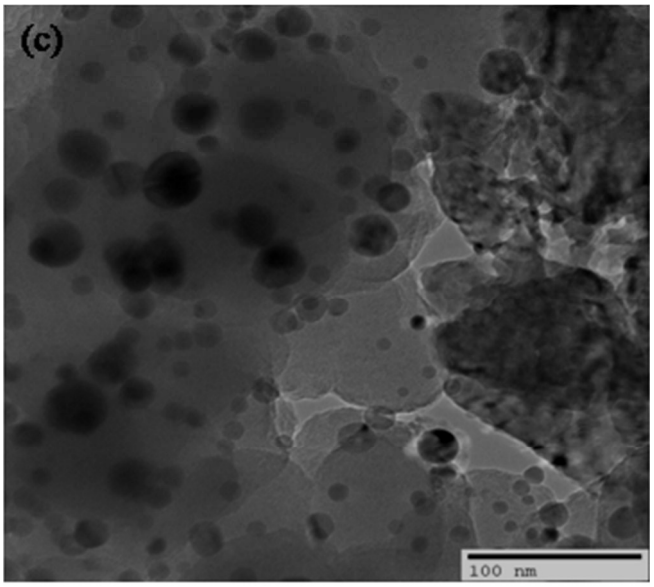

Fig. 14. TEM micrographs of native HEWL (a), HEWL + 12-E2-12 (b), and HEWL + 14-E2-14 (c); [HEWL] = 20 μM, [12-E2-12] and [14-E2-14] = 1.13mM.

4. Conclusions

In this research article, the interactions between two green gemini surfactants (*m*-E2-*m*) with hen white egg lysozyme (HEWL) have been examined using spectroscopic, calorimetric, microscopic and molecular docking techniques. The biophysical parameters depicted efficient binding of *m*-E2-*m* to HEWL. The experimental (UV and fluorescence) results also indicate that the quenching of fluorescence of HEWL by *m*-E2-*m* geminis is of static nature. The CD and TEM results indicate that the secondary structure of HEWL molecules changes in the presence of *m*-E2-*m*. ITC results validate the contribution of hydrophobic as well as electrostatic forces governing the interaction. The molecular docking results confirm the binding of *m*-E2-*m* residues in the proximity of predominant fluorophores (Trp-108/Trp-62). Moreover, Trp-123 was also found in the proximity of 12-E2-12 which advocates its contribution in fluorescence quenching.

View Article Online
DOI: 10.1039/C5RA20576J

Since surfactants as well as lysozyme are used in many pharmaceutical compilations, we believe that this article in future may help to understand the role of *m*-E2-*m* biodegradable surfactants as excipients in pharmaceutical and drug delivery related purposes.

Acknowledgements

IAB is thankful to UGC, New Delhi, India for BSR fellowship. The authors also thank University Sophisticated Instruments Facility (USIF), Aligarh Muslim University, for TEM studies.

References

1 M. N. Jones, *Chem. Soc. Rev.*, 1992, **42**, 127.

2 E. D. Goddard and K. P. Ananthapadmanabhan, *Interactions of Surfactants with Polymers and Proteins*, CRC Press, Inc., London, UK, 1993.

3 A. Stenstam, D. Topgaard and H. Wennerstrom, *J. Phys. Chem. B,* 2003, **107**, 7987–7992.

4 Y. Li, X. Wang and Y. Wang, *J. Phys. Chem. B,* 2006, **110**, 8499–8505.

5 J. M. Jung, G. Savin, M. Pouzot, C. Schmitt and R. Mezzenga, *Biomacromolecules*, 2008, **9**, 2477–2486.

6 R. Das, D. Guha, S. Mitra, S. Kar, S. Lahiri and S. Mukherjee, *J. Phys. Chem. A,* 1997, **101**, 4042–4047.

7 R. C. Lu, A. N. Cao, L. H. Lai and J. X. Xiao, *J. Colloid Interface Sci*., 2006, **299**, 617–625.

View Article Online
DOI: 10.1039/C5RA20576J

8 E. Blanco, P. Messina, J. M. Ruso, G. Prieto and F. Sarmiento, *J. Phys. Chem. B*, 2006, **110**, 11369–11376.

9 A. J. Kirby, P. Camilleri, J. B. F. N. Engberts, M. C. Feiters, R. J. M. Nolte, O. Söderman, M. Bergsma, P. C. Bell, M. L. Fielden, C. R. G. Rodríguez, P. Guedat, A. Kremer, C. McGregor, C. Perrin, G. Ronsin and M. C. P. van Eijk, *Angew. Chem*., 2003, **42**, 1448–1457.

10 A. Bajaj, B. Paul, S. S. Indi, P. Kondaiah and S. Bhattacharya, *Bioconjug. Chem*., 2007, **18**, 2144–2158.

11 L. Caillier, E. T. de Givenchy, R. Levy, Y. Vandenberghe, S. Geribaldi and F. Guittard, *J. Colloid Interface Sci*., 2009, **332**, 201–210.

12 C. Bombelli, G. Caracciolo, P. D. Profio, M. Diociaiuti, P. Luciani, G. Mancini, C. Mazzuca, M. Marra, A. Molinari, D. Monti, L. Toccacieli and M. Venanzi, *J. Med. Chem*., 2005, **48**, 4882–4891.

13 J. Cross, *Environmental Aspects of Cationic Surfactants*, in: J. Cross, and E. J. Singer (eds.), *Cationic Surfactants*, Marcel Dekker, New York, 1994.

14 N. Funasaki, M. Ohigashi, S. Hada and S. Neya, *Langmuir*, 2000, **16**, 383–388.

15 L. Huber, L. Nitschke, *Environmental Aspects of Surfactants*, in: K. Holmberg, (ed.), *Handbook of Applied Surface and Colloidal Chemistry*, Wiley, Chichester, England, 2002.

16 A. R. Tehrani-Bagha, H. Oskarsson, C. G van Ginkel and K. Holmberg, *J Colloid Interface Sci*., 2007, **312**, 444-452.

17 A. Ghosh, K. V. Brinda and S. Vishveshwara, *Biophysical J.*, 2007, **92**, 2523–2535.

View Article Online
DOI: 10.1039/C5RA20576J

18 A. B. Khan, M. Ali, N. A. Malik, A. Ali and R. Patel, *Colloids Surf. B*, 2013, **112**, 460–465.

19 G. Paramaguru, A. Kathiravan, S. Selvaraj, P. Venuvanalingam and R. Renganathan, *J. Hazard. Mater.*, 2010, **175**, 985–991.

20 A. S. Antipova, M. G. Semenova, L. E. Belyakova and M. M. Il'n, *Colloids Surf. B,* 2001, **21**, 217–230.

21 G. A. vanAken, T. B. J. Blijdenstein and N. E. Hotrum, *Curr. Opin. Colloid Interface Sci*., 2003, **8**, 371–379.

22 L. Kong, J. K. Beattie and R. J. Hunter, *Colloids Surf., B*, 2003, **27**, 11–21.

23 R. J. Zana, *Colloid Interface Sci.,* 2002, **248**, 203–220.

24 J. C. Rochet and P. T. Lansbury Jr, *Curr. Opin. Struct. Biol*, 2000, **10**, 60–68.

25 Y. Han, C. He, M. Cao, X. Huang, Y. Wang, and Z. Li, *Langmuir,* 2010, **26**, 1583–1587.

26 Z. Yaseen, S. Rehman, M. Tabish, A. H. Shalla and Kabir-ud-Din, *RSC Adv.,* 2015, **5**, 58616–58624.

27 N. J. Turro, X. G Lei, *Langmuir,* 1995, **11**, 2525−2533.

28 S. Ghosh, A. A. Banerjee, *Biomacromolecules,* 2002, **3**, 9−16

29 Y. Pi, Y. Shang, C. Peng, H. Liu, Y. Hu and J. Jiang, *Biopolym.,* 2006, **83**, 243–249.

30 M. U. H. Mir, J. K. Maurya, S. Ali, S. Ubaid-Ullah, A. B. Khan and R. Patel, *Process Biochem*., 2014, **49**, 623–630.

31 Y. S. Wang, R. Guo and J. Xi, *J. Colloid Interface Sci.* 2009, **331**, 470−475.

32 D. Wu, G. Y. Xu, Y. J. Feng, Y. J. Wang and Y. Y. Zhu, *Colloid Polym. Sci.,* 2009, **287,** 225–230.

View Article Online
DOI: 10.1039/C5RA20576J

33 N. Gull, P. Sen, R. H. Khan and Kabir-ud-Din, *J. Biochem*., 2009, **145**, 67–77.

34 N. Gull, P.Sen, R. H. Khan and Kabir-ud-Din, *Langmuir*, 2009, **25**, 11686–11691.

35 M. A. Mir, J. M. Khan, R. H. Khan, A. A. Dar and G. M. Rather, *J. Phys. Chem. B,* 2012, **116**, 5711–5718.

36 M. A. Mir, J. M. Khan, R. H. Khan, G. M. Rather and A. A. Dar, *Colloids Surf. B*, 2010, **77**, 54–59.

37 V. I. Martín, A. Rodríguez, A. Maestre and M. L. Moya, *Langmuir, 2*013, **29**, 7629−7641.

38 Y. Ge, S. Tai, Z. Xu, L. Lai, F. Tian, D. Li, F. Jiang, Y. Liu, and Z. Gao, *Langmuir,* 2012, **28**, 5913−5920

39 M. Akram, I. A. Bhat and Kabir-ud-Din, *Int. J. Biol. Macromol.*, 2015, **78**, 62–71.

40 M. Akram, I. A. Bhat, W. F. Bhat and Kabir-ud-Din, *Spectrochim. Acta Part A*, 2015, **150**, 440–450.

41 M. Akram, I. A. Bhat and Kabir-ud-Din, *J. Lumin.,* (accepted).

42 J. Tang, F. Luan and X. Chen. *Bioorg. Med. Chem.,* 2006, **14**, 3210–3217.

43 W. C. Abert, W. M Gregory and G. S.Allan, *Anal Biochem.,* 1993, **213**, 407–413.

44 Q. Saquib, A. Al-Khedhairy, S. A Alarifi, S. Dwivedi, J. Mustafa and J. Musarrat. *Int. J .Biol. Macromol*., 2010, **47**, 60–67.

45 D. Mustard and D.W. Ritchie, *Proteins: Struct. Funct. Bioinf*., 2005, **60,** 269-274.

46 W. L. DeLano, *The PyMOL Molecular Graphics System*, DeLano Scientific, San Carlos, CA, USA, 2002.

47 R. Patel, J. K. Maurya, M. U. H. Mir, M. Kumari and N. Maurya, *J. Lumin*., 2014, **154**, 298–304.

View Article Online
DOI: 10.1039/C5RA20576J

48 J. R. Lakowicz, *Principles of Fluorescence Spectroscopy*, 2nd ed., Plenum: New York, 1999, 239−240.

49 W. R. Ware, *J. Phys. Chem.,* 1962, **66,** 455-458.

50 Y. Wang, X. Jiang, L. Zhou, L. Yang, G. Xia, Z. Chen and M. Duan, *Colloids and Surfaces A,* 2013,***436***, 1159–1169

51 G. W. Zhang, Q. M. Que, J. H. Pan and J. B. Guo, *J. Mol. Struct*., 2008, **881**, 132−138.

52 U. S. Mote, S. L. Bhattar, S. R. Patil and G. B. Kolekar, *Lumin.*, 2010, **25**, 1−8.

53 J. Q. Lu, F. Jin, T. Q. Sun and X. W. Zhou, *Int. J. Biol. Macromol*., 2007, **40**, 299–304.

54 C. Barakat and D. Patra, *Lumin.,*2013, **28**, 149−155.

55 T. Asakawa, T. Okada, T. Hayasaka, K. Kuwamoto, A. Ohta, S. Miyagishi, *Langmuir*, 2006, **22**, 6053−6055.

56 N. Shahabadi and M. Maghsudi, *Mol. BioSyst.,* 2014, **10**, 338−347.

57 D. Patra and C. Barakat, *Int. J. Boil. Macromol*., 2012, **50**, 885–890.

58 H. Chen, S. S. Ahsan, M. B. Santiago-Berrios, H. D. Abruna and W. W. Webb, *J. Am. Chem. Soc.,* 2010, **132**, 7244–7245.

59 F. F. Tian , F. L. Jiang , X. L. Han , C. Xiang , Y. S. Ge , J. H. Li , Y. Zhang, R. Li , X. L. Ding and Y. Liu**,** *J. Phys. Chem. B,* 2010, **114***,* 14842–14853.

60 B. K. Sahoo, K. S. Ghosh and S. Dasgupta, *Biopolym.,* 2008, **91**, 108−119.

61 N. Shahabadi and S. Hadidi, *Spectrochim. Acta Part A.*, 2014, **122,** 100−106.

62 Y. Shu , M. Liu , S. Chen , X. Chen and J. Wang**,** *J. Phys. Chem. B*, 2011, **115,** 12306–12314.

63 N. Keswani and N. Kishore, *J. Chem. Therm.,* 2011, **43**, 1406−1413.

64 X. Diaz. E. Abuin and E. Lissi,. *J. Photochem. Photobiol. A*, 2003, **155**, 157−162.

View Article Online
DOI: 10.1039/C5RA20576J

65 N. J. Faergeman, B. W. Sigurskjold, B. B. Kragelund, K.V. Andersen and J. Knudsen, *Biochemistry, 1*996, **35**, 14118−14126.

66 J. Rosendal, P. Ertbjerg and J. Knudsen, *Biochem. J*. 1993, **290**, 321−316.

67 M. Akram, I. A. Bhat, S. Anwar, Kabir-ud-Din, *J. Mol. Liquids*, 2015, **212**, 641-649.

68 X. Zhao, R. Liu, Z. Chi, Y. Teng, and P. Qin, *J. Phys. Chem. B,* 2010**, *114,*** 5625−5631.

69 X. Zhao, F. Sheng, J. Zheng, and R. Liu, *J. Agric. Food Chem*. 2011, **59**, 7902−7909

70 X. Zhao, F. Hao, D. Lu, W. Liu, Q. Zhou and G. Jiang, *ACS Appl. Mater. Interfaces*, 2015, **7**, 18880−18890.

71 X. Zhao, R. Liu, Y. Teng and X. Liu, *Sci. Total Environ.,* 2011, **409**, 892−897.

72 X. Zhao, D. Lu, F. Hao and R. Liu, *J. Harazard. Mater*., 2015, **292**, 98−107.

View Article Online
DOI: 10.1039/C5RA20576J

TOC

Different binding pattern of *m*-E2-*m* (12-E2-12 and 14-E2-14) surfactants to HEWL